

THE CN RADICAL IN DIFFUSE INTERSTELLAR CLOUDS¹S. R. FEDERMAN,^{2,3} A. C. DANKS,⁴ AND D. L. LAMBERT²

Received 1984 February 27; accepted 1984 June 14

ABSTRACT

A survey of 15 lines of sight for the CN $B^2\Sigma^+-X^2\Sigma^+$ interstellar absorption lines shows that the CN column density in diffuse interstellar clouds follows the relation $\log N(\text{CN}) \propto m \log N(\text{H}_2)$, where $m \approx 3$. This result is reproduced by a reaction network in which CN is produced primarily from C_2 by the neutral-neutral reaction $\text{C}_2 + \text{N} \rightarrow \text{CN} + \text{C}$, and photodissociation is the main destruction pathway for the neutral molecules CH, C_2 , and CN. The CN radical is the first molecular species observed in diffuse clouds that requires a neutral-neutral reaction for its formation in the gas phase. The network also reproduces the observed ratio $N(\text{CN})/N(\text{H}_2)$.

Subject headings: interstellar: molecules — molecular processes

I. INTRODUCTION

Molecules residing in diffuse interstellar clouds reflect the physical and chemical processes occurring within the clouds. The CN radical's rôle as a monitor of the cosmic microwave 3 K emission is well known and understood (see Thaddeus 1972). By contrast, the chemistry of this radical has not been studied in detail for an ensemble of diffuse clouds open to analysis by optical spectroscopy. The present paper attempts to repair this observational and theoretical omission.

Our observations of CN absorption lines along lines of sight with a known column density of molecular hydrogen were intended to establish the outlines of the reaction network controlling the equilibrium density of CN. A similar program for the CH radical showed that ion-molecule reactions beginning with $\text{C}^+ + \text{H}_2 \rightarrow \text{CH}_2^+ + h\nu$ were responsible for the formation of CH and that photodissociation and the ion molecule reaction $\text{CH} + \text{C}^+ \rightarrow \text{C}_2^+ + \text{H}$ were the dominant destruction routes (Federman 1982; Danks, Federman, and Lambert 1984). These recent surveys of CH lines established the tight correlation of CH with H_2 and the absolute level of the CH column densities as predicted by the reaction network first sketched by Black and Dalgarno (1973) and Black, Dalgarno, and Oppenheimer (1975). A complementary program for CO was undertaken by Federman *et al.* (1980). They found that CO also forms in gas with a large H_2 content. The pathway leading to CO includes the reactions $\text{H}^+ + \text{O} \rightarrow \text{O}^+ + \text{H}$ and $\text{O}^+ + \text{H}_2 \rightarrow \text{OH}^+ + \text{H}$, which leads to formation of OH, and $\text{C}^+ + \text{OH} \rightarrow \text{CO}^+ + \text{H}$; the major destruction mechanism for OH and CO is photodissociation (see also Glassgold and Langer 1976).

Our observational exploration of the correlation between CN and H_2 was prompted both by the paucity of published observations of interstellar CN lines and by the realization that nitrogen is predominantly neutral, in contrast to carbon and oxygen which can be present as ions in the diffuse interstellar gas. This difference in the degree of ionization, which reflects the ordering of the ionization potentials of the atoms [i.e.,

$I(\text{N}) > I(\text{H})$, but $I(\text{C})$ and $I(\text{O}) \lesssim I(\text{H})$] may be expected to be reflected in the chemistry of CN and the CN- H_2 correlation. Our observations provide this correlation (§ IIIa and Fig. 3). In § III, we propose a reaction network which reproduces the observed correlation.

II. OBSERVATIONS AND RESULTS

High-resolution spectra near 3875 Å were obtained for 15 stars drawn from a sample of reddened stars with known column densities of H_2 (Bohlin, Savage, and Drake 1978).

Eleven stars were observed at the European Southern Observatory in observing runs in 1983 February and May with the 1.4 m coude echelle spectrometer (Enard 1979). With a 1872 element Reticon array as a detector, the spectrometer centered at 3879 Å provided a 30 Å spectral interval at a resolving power of 74,250. A wavelength calibration was provided by an observation of a thorium hollow cathode lamp. Diode-to-diode differences of sensitivity were removed by observing the continuous spectrum of a quartz-halogen lamp. A majority of the stars were observed repeatedly and individual spectra co-added to increase the signal-to-noise ratio. All observations were reduced with the Image Handling and Processing System (IHAP) written for ESO by Middleburg (1981). A spectrum of χ Oph is shown in Figure 1.

Four stars in the northern Milky Way were observed in 1983 November at the McDonald Observatory with the 2.7 m telescope's coude echelle spectrometer and a 936 element self-scanned Digicon (Tull, Choisser, and Snow 1975). A 17 Å spectral interval centered at 3880 Å was recorded at a resolving power of 50,000. Wavelength calibration was provided by an observation of an iron-neon hollow cathode lamp. Diode-to-diode variations in sensitivity were measured by observing a quartz-halogen lamp.

Our spectra cover the three interstellar CN lines $R(0)$, $R(1)$, and $P(1)$ from the 0-0 band of the violet ($B^2\Sigma^+-X^2\Sigma^+$) system. We give in Table 1 the equivalent width (W_λ) of the $R(0)$ line. Upper limits to W_λ correspond to the 2σ limit based on the error in the continuum. Our results are in quite good agreement with published values—see Table 1. In particular, our measurements for ζ Oph are consistent with the accurate measurements recently reported by Meyer and Jura (1984). The W_λ 's of the three lines measured in ρ , χ , and ζ Oph are consis-

¹ Based in part on observations collected at the European Southern Observatory, La Silla, Chile.

² Department of Astronomy, University of Texas, Austin, Texas.

³ Jet Propulsion Laboratory, California Institute of Technology, Pasadena, California.

⁴ European Southern Observatory, Santiago, Chile.

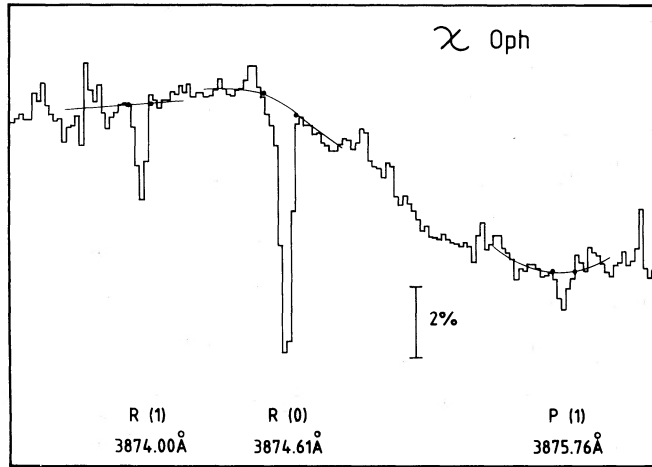


FIG. 1.—Interstellar CN lines in the spectrum of the Be star χ Oph. The R(0) and R(1) lines are superposed on a broad Balmer emission line. Thin lines show the adopted local continua, and the solid circles define the limits of integration for the W_λ estimates.

tent with an excitation temperature near 3 K—see the W_λ 's given in a footnote to Table 1.

A check on the photometric accuracy of the measured W_λ 's is offered by the CH $B^2\Sigma-X^2\Pi$ 0-0 lines which appear just to the red of the CN lines. The 3886 Å $Q_2(1) + {}^2R_{12}(1)$ doublet is the strongest of the three CH lines. This doublet's predicted W_λ is provided from the observed W_λ of the $A^2\Delta-X^2\Pi$ system's 4300.3 Å $R_2(0)$ Λ -doublet and the laboratory measurements of the $A-X$ and $B-X$ oscillator strengths (see Lambert 1978; Danks, Federman, and Lambert 1984). We correct the W_λ 's, when necessary, for saturation by adopting a Doppler parameter $b = 1 \text{ km s}^{-1}$ and the Strömberg (1948) curve of growth. This calculation is based on the approximation (see below) that the separation of the doublets' components is effectively small.⁵ The W_λ of the 4300.3 Å line is taken from Danks, Federman, and Lambert (1984) for all of our program stars except κ Cas, ζ Per, κ Aql, and 68 Cyg, where the observed W_λ given by Federman (1982) is adopted. Figure 2 shows that the predicted and observed W_λ 's of the 3886 Å doublet are tightly correlated. The least squares fit to the detections of the 3886 Å line shows that the observed W_λ 's are $87\% \pm 10\%$ (correlation coefficient $r^2 \approx 0.93$) of the predicted W_λ . This 13% difference could easily reflect an error in the adopted oscillator strengths; Lambert (1978) estimated the oscillator strength of the $B-X$ system to be uncertain by about $\pm 10\%$.

Predicted W_λ 's in Figure 2 for the three strongest lines are also sensitive to the adopted b value. For the ζ Oph clouds, a typical example, published b values are about 1 km s^{-1} ; for example, $b = 1.3 \pm 0.1 \text{ km s}^{-1}$ from an analysis of the profile of the CN R(0) line (Hegyí, Traub, and Carleton 1972) and $b = 1.5 \pm 0.3 \text{ km s}^{-1}$ from an application of the doublet method to the Ca II H and K lines (Herbig 1968). However, there is evidence that many individual cloudlets are characterized by a much smaller Doppler parameter: $b \approx 0.5 \text{ km s}^{-1}$ according to Blades, Wynne-Jones, and Wayte (1980), and

⁵ Competing definitions of b values exist and are not always distinguished. The normalized velocity distribution $\psi(v) = \exp(-v^2/b^2)/(\pi^{1/2}/b)$ defines our b value (see Strömberg 1948). If a dispersion (σ) is preferred, $2\sigma^2 = b^2$ or $\sigma = b/2^{1/2}$. Authors may quote the width of an optically thin line provided by such a distribution. If b_{line} is the FWHM of the line, $b_{\text{line}} = 2(\ln 2)^{1/2}b = (8 \ln 2)^{1/2}\sigma$.

Liszt suggested $b \lesssim 0.3 \text{ km s}^{-1}$ for gas near ζ Oph from observations of the CO 2.6 mm and CH 9 cm lines.

The two components of the 4300 Å are split by about 1.4 km s^{-1} , so that if $b = 0.5 \text{ km s}^{-1}$, their overlap is extremely small. For the 3886 Å doublet, we estimate the separation to be about 0.7 km s^{-1} , and the components' overlap is reduced significantly for $b = 0.5 \text{ km s}^{-1}$. Sample calculations for limiting cases suffice to demonstrate that adoption of the lower b value has a small effect on the conclusions drawn from Figure 2. The 4300.3 Å close doublet samples the lower levels $T_{2e}(J = \frac{1}{2})$ and $T_{2f}(J = \frac{1}{2})$. On the other hand, the 3886 Å doublet originates from the upper level, $T_{2f}(\frac{1}{2})$. We assume that the two levels are equally populated. We consider χ Oph with $W_\lambda(4300 \text{ Å}) = 23 \text{ mÅ}$. If $b = 1 \text{ km s}^{-1}$ and the components of each doublet are assumed coincident, we predict $W_\lambda(3886 \text{ Å}) = 8.0 \text{ mÅ}$ and observe $W_\lambda(3886 \text{ Å}) = 6.1 \text{ mÅ}$. The predicted value is reduced to 6.8 mÅ if the components at 4300 Å are considered fully resolved. If $b = 0.5 \text{ km s}^{-1}$ and both doublets are taken to be resolved, the predicted value is 7.2 mÅ . Two conclusions follow. First, recognition that the CH lines are close doublets improves the agreement between the predicted and observed $W_\lambda(3886 \text{ Å})$'s even if $b = 1 \text{ km s}^{-1}$. Second, this agreement is insensitive to the choice of the b value in the range $b \gtrsim 0.4 \text{ km s}^{-1}$.

The primary lesson to be drawn from Figure 2 is that our spectra which provide the CN equivalent width measurements and upper limits also provide W_λ 's for CH lines which are in excellent agreement with the predicted values. Figure 2 shows that accurate measurements are possible to at least the $W_\lambda \approx 0.5 \text{ mÅ}$ level on most of our spectra. The two most discordant points refer to κ Aql and 68 Cyg and are based on W_λ 's for the 4300.3 Å line from Federman (1982). A comparison of W_λ 's from Danks, Federman, and Lambert (1984) and Federman (1982) for five stars in common shows that while the former span the range 1.6–4.9 mÅ, the latter are compressed into the narrower interval of 2.8–4.9 mÅ. There is a hint here that Federman may have overestimated the W_λ 's of the weak CH

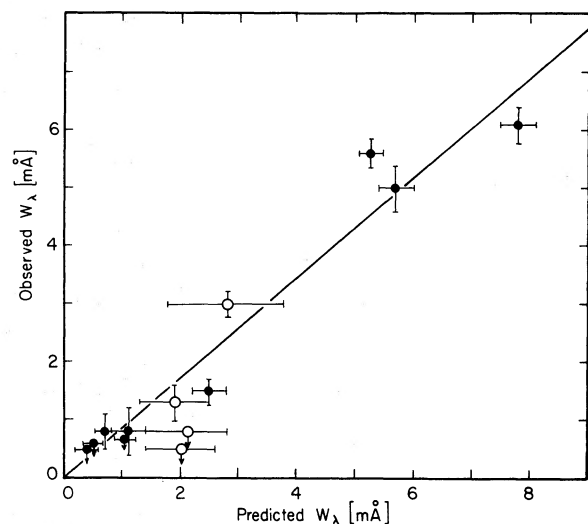


FIG. 2.—Observed and predicted equivalent widths for the CH $B^2\Sigma-X^2\Pi$ $Q_2(1) + {}^2R_{12}(1)$ line at 3886 Å. Predictions based on W_λ 's for the 4300.3 Å line measured by Danks, Federman, and Lambert (1984) are given by the filled circles. Four estimates based on W_λ 's from Federman (1982) are shown by the open circles.

TABLE 1
CN, H₂, AND H I DIFFUSE CLOUDS

STAR		$W_\lambda(3874.6 \text{ \AA})$ (mÅ)		LOG $N(\text{CN})$	LOG $N(\text{H}_2)^a$	LOG $N(\text{H I})^a$
HD	Name	This Paper	Published Results	(cm^{-2})	(cm^{-2})	(cm^{-2})
2905	κ Cas	≤ 0.6	...	≤ 11.29	20.28	21.20
22951	40 Per	≤ 0.8	...	≤ 11.41	20.46	21.10
23180	o Per	...	7.5 ^b	12.42	20.61	20.90
24398	ζ Per	...	10.0 ^b , 9.1 \pm 0.9 ^c	12.59	20.67	20.81
24912	ξ Per	0.8 \pm 0.2	< 1 _b	11.41	20.53	21.11
112244	...	≤ 1.0	...	≤ 11.50	20.14	21.08
143275	δ Sco	≤ 0.4	...	≤ 11.11	19.41	21.15
144217A	β^1 Sco	≤ 0.4	...	≤ 11.11	19.83	21.09
147165	σ Sco	≤ 0.4	...	≤ 11.11	19.79	21.34
147933	ρ Oph A	5.9 \pm 0.3 ^d	...	12.30	20.57	21.81
148184	χ Oph	4.0 \pm 0.5 ^d	< 3 ^e	12.12	20.63	21.15
149038	μ Nor	≤ 0.6	...	≤ 11.29	20.44	21.00
149757	ζ Oph	7.5 \pm 0.3 ^d	7.6 \pm 0.3 ^f	12.42	20.64	20.72
164353	67 Oph	≤ 0.5	...	≤ 11.20	20.26	21.00
167264	15 Sgr	≤ 0.8	...	≤ 11.41	20.28	26.15
184915	κ Aql	≤ 0.7	...	≤ 11.35	20.31	20.90
203064	68 Cyg	≤ 0.6	...	≤ 11.29	20.30	21.00
210839	λ Cep	...	7.0 ^g	12.39	20.78	21.11

^a Bohlin *et al.* 1978.

^b Chaffee 1974.

^c Clauser and Thaddeus 1972.

^d W_λ 's for $R(1)$ and $P(1)$ are 1.2 and 0.5 mÅ in χ Oph, 2.6 and 1.2 mÅ in ζ Oph, and 2.5 and 1.2 mÅ in ρ Oph A.

^e Frisch 1979.

^f This value is from Hegyi, Traub, and Carleton 1972 and a PEPSIOS spectrum. Other published values include $W_\lambda = 9.2$ mÅ (Herbig 1968), 8.4 Å (Bortolot, Clauser, and Thaddeus 1969), 6.6 \pm 0.3 mÅ (Clauser and Thaddeus 1972), and an accurate measurement $W_\lambda = 7.43 \pm 0.10$ mÅ (Meyer and Jura 1984).

^g Chaffee and Dunham 1979.

lines. Spectra considered by Danks *et al.* were of superior quality and should clearly be given higher weight.

The line of sight column density of CN molecules in the lowest rotational level $N'' = 0$ was computed from the W_λ of the 3874.6 Å line using the absorption oscillator strength $f_{\text{line}} = 0.0342$ (see the Appendix). The line is an unresolved blend of the $R_1(0)$ and $^RQ_{21}(0)$ lines with the former having an oscillator strength twice that of the satellite line. The Ström-gren (1948) curve of growth with $b = 1$ km s⁻¹ was used to estimate the small corrections for saturation of the stronger CN lines; the correction is 20% for $W_\lambda = 10$ mÅ. The total CN column density was computed from $N(N'' = 0)$ assuming an excitation temperature of 2.8 K, when the excited state population is $N(N'' = 1)/N(N'' = 0) = 0.43$ and $N(N'' = 2)/N(N'' = 0) = 0.015$. We assumed that the levels comprising the fine and hyperfine structure are in thermal equilibrium at the 2.8 K temperature of the cosmic microwave flux. If $b = 0.5$ km s⁻¹ is preferred, an approximate lower bound to observed values for our lines of sight, the CN column densities are increased by a maximum of 20% for $W_\lambda = 10$ mÅ to 13% at $W_\lambda = 5$ mÅ over the values in Table 1. These estimates provide an upper limit because there is a 0.3 km s⁻¹ separation between the two components— $^RQ_{21}$ and R_1 —of the $R_1(0)$ line and this separation necessarily delays the onset of separation. The major source of uncertainty affecting the total column density $N(\text{CN})$ is in the measurement of the equivalent widths.

III. CN CHEMISTRY IN DIFFUSE CLOUDS

a) CN, H₂ and H I

A powerful clue to the chemistry of CN in diffuse clouds is offered by the comparison of the CN column density with the

column densities of H₂ and H I along the same lines of sight—see Figure 3. In these comparisons, we include published results for o Per, ζ Per, and λ Cep (Chaffee 1974; Chaffee and Dunham 1979). Other measurements of interstellar CN lines may be found in the literature (see below), but direct measurements of the H₂ and H I column densities are unavailable. Figure 3 shows that the CN column density for our sample is a steep function of the H₂ column density and is quite uncorrelated with the H I column density. The relation $\log N(\text{CN}) \propto m \log N(\text{H}_2)$, where $m \approx 3$, is a reasonable fit to the points. For the detections shown in Figure 3, a least squares fit yields $m \approx 3.0 \pm 1.8$ with $r^2 \approx 0.37$. If the additional data plotted in Figure 5 are included (see below for details), then the fit becomes $m \approx 3.0 \pm 0.5$ with $r^2 \approx 0.77$. The larger data set has better statistics because of the expanded range in both $N(\text{CN})$ and $N(\text{H}_2)$. A somewhat larger value for m is possible because the observed amount of CN toward directions where we quote upper limits may be significantly below our limits. With the present paucity of points with $\log N(\text{CN}) \leq 12$, we cannot exclude the possibility that the CN column density increases abruptly at $\log N(\text{H}_2) \approx 20.5$ and then increases with $m \approx 3$ for $\log N(\text{CN}) \gtrsim 12$; an abrupt increase could arise if photodissociation of CN occurs through absorption of ultraviolet line radiation. However, it seems more reasonable that the $N(\text{CN})$ versus $N(\text{H}_2)$ relation be continuous as is indicated by the models. The steep dependence of $N(\text{CN})$ on $N(\text{H}_2)$ contrasts with the cases of other carbon-bearing molecules where $N(\text{CH})$ varies linearly with $N(\text{H}_2)$ (Federman 1982; Danks, Federman, and Lambert 1984) and where $N(\text{CO})$ varies at most quadratically with $N(\text{H}_2)$ (Federman *et al.* 1980).

Our discussion of the chemistry begins with a sketch showing how a molecule's density is related to the gas density

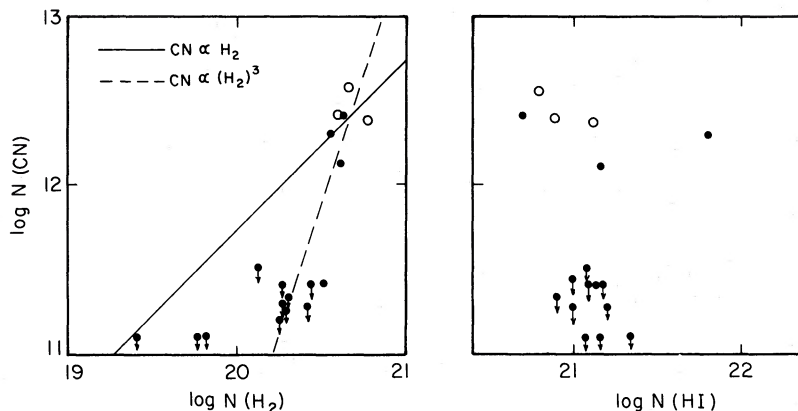


FIG. 3.—A comparison of the CN column density with the (left) H_2 and (right) $H\ I$ column densities given by Bohlin, Savage, and Drake (1978); column densities are expressed in the units cm^{-2} . Note that $N(\text{CN}) \propto N(H_2)^3$ is a reasonable fit to the data points (filled circles denote the new observations, and open circles, the previously published observations for σ Per, χ Per, and λ Cep.)

for simple linear reaction pathways. First, consider the molecule AH formed by $A + H_2 \rightarrow AH + H$ with AH destroyed by photodissociation; the equilibrium density $n(AH)$ may be written

$$n(AH) = n(A)n(H_2)k_{AH}/G_{AH} = x(A)n(H_2)n_{AH}/G_{AH} \text{ cm}^{-3},$$

where k_{AH} is the bimolecular rate constant and G_{AH} is the photodissociation rate, which is itself related to the cloud density and size and might be written as $G_{AH} = G_{AH}^0 \exp(-\tau_{AH})$ with τ_{AH} being a mean optical depth in the ultraviolet. The concentration of species A is $x(A)$; $x(A) = n(A)/n$.

If the reaction $AH + A \rightarrow A_2 + H$, a minor competitor to photodissociation of AH , is included and is followed by $A_2 + B \rightarrow AB + A$ with photodissociation of both A_2 and AB as the leading destructive processes for these molecules, the equilibrium density of AB may be written

$$n(AB) = x(A)^2 x(B) n(H_2) n^3 (k_{AH}/G_{AH})(k_{A_2}/G_{A_2})(k_{AB}/G_{AB}) \text{ cm}^{-3}. \quad (1)$$

Clearly, the molecule AB , which we term a third-generation molecule, has a steeper dependence on the gas density and optical depth than AH , a first-generation molecule. In particular, $n(AB)$ is proportional to $n^3 n(H_2) \exp(3\tau)$ for $\tau_{AH} \approx \tau_{AB} \approx \tau_{A_2} \approx \tau$. The exponential factor involving τ plays an especially important role causing $n(AB)$ to vary much more rapidly than $n(H_2)$, and leading to a steep dependence of AB on H_2 . On the other hand, differences in temperature play a minor rôle because (1) exothermic ion-molecule reactions are not temperature sensitive, and (2) exothermic neutral-neutral reactions involving a radical and an atom vary weakly with temperature ($T^{1/2}$). The precise form of the molecule's dependence on the gas density and optical depth depends on the construction of the reaction pathway. For example, if the reaction $AH + A \rightarrow A_2 + H$ replaces photodissociation of AH as the leading destructive process for AH , we find

$$n(AB) = x(A)x(B)n(H_2)n^2(k_{AH}/G_{A_2})(k_{AB}/G_{AB}) \text{ cm}^{-3}.$$

Similarly, closed loops within the reaction pathway may modify the dependence on the gas density and optical depth. Nonetheless, molecules formed after several steps of gas phase reactions involving neutral molecules will be expected to vary more steeply with the H_2 density in at least the diffuse clouds

where photodissociation can compete with bimolecular reactions in the destruction of a molecule.

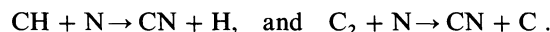
The very steep increase of the CN density with H_2 density suggests that CN is probably a third-generation molecule. This status surely reflects the fact that atomic N is neutral in diffuse clouds. In the following subsections, we discuss the production and destruction of CN in such clouds.

b) Production of CN

Gas phase channels for CN production have been described in the literature (cf. Prasad and Huntress 1980). The initiating steps for the principal channels are the ion-molecule reactions



and the neutral-neutral reactions



The two ion-molecule schemes proceed via hydrogen abstraction:



Electron dissociative recombination of HCN^+ and H_2CN^+ leads to neutral products, including CN. Since the branching ratios for the neutral products are generally not known, each dissociative branch is assumed to have equal probability.

A major problem with the ion-molecule scheme is that at a kinetic temperature of $\lesssim 70$ K, very little NH or CH^+ forms in a diffuse cloud (cf. Prasad and Huntress 1980). The formation of NH is inhibited by the small amount of ionized nitrogen present in neutral diffuse clouds. In the gas phase NH is produced by hydrogen abstraction reactions, such as $N^+ + H_2 \rightarrow NH^+ + H$, and electron dissociative recombination of NH_2^+ and NH_3^+ . The production of NH in the gas phase is thus limited by the amount of N^+ present. Production of CH^+ is low because of the endothermicity of the reaction $C^+ + H_2 \rightarrow CH^+ + H$. Rate constants for the ion-molecule reactions participating in the production of CN are now known to be considerably smaller than estimated previously (Viggiano *et al.* 1980). If there were no alternative production channels for NH or CH^+ , the channel for CN production with the neutral-neutral reactions would be at least a factor of 10 faster than the ion-molecule channels.

However, ion-molecule channels cannot be dismissed quite so readily because the observed abundance of CH^+ along lines of sight through diffuse clouds exceeds the predicted abundance. The CH^+ is thought to reside in hot shocked gas (Elitzur and Watson 1978, 1980). There is direct observational evidence that the higher CH^+ abundance does not result in significant production of CN. In certain lines of sight, the radial velocity of the CH^+ differs markedly from that provided by the neutral molecules with the CN line matching the velocity of the CO and CH lines, not that of the CH^+ line (Dickman *et al.* 1983). A low density of CN in the shocked gas contributing to the CH^+ line is expected because (i) the shock is optically thin and photodissociation destroys molecules, (ii) the shocked gas is of low density, and (iii) most probably, molecular hydrogen is a minor constituent. Our estimate is that less than 10% of the CN is formed in the shocked gas. This estimate might be checked by obtaining accurate profiles of the CN, CH, and CH^+ lines for a line of sight with CH and CH^+ at different radial velocities.

Production efficiency for CN in the ion-molecule scheme is enhanced if NH is formed on the surface of grains. Crutcher and Watson (1976) made measurements of OH and NH toward α Persei to determine the importance of grain formation for NH. Their upper limit $N(\text{NH}) \leq 7 \times 10^{11} \text{ cm}^{-2}$ indicates that the formation of NH on grain surfaces is unlikely. The upper limit of Crutcher and Watson cannot be used with confidence in the ion-molecule channel for CN production involving NH because if grain formation is unimportant, the expected value of $N(\text{NH})$ from gas-phase reactions is significantly less than $7 \times 10^{11} \text{ cm}^{-2}$.

The two dominant pathways for CN production with neutral-neutral reactions are $\text{CH} + \text{N}$ and $\text{C}_2 + \text{N}$. The observed steep dependence of CN on H_2 suggests that the second neutral-neutral reaction is the more important one. The rate constant for $\text{CH} + \text{N}$ at 298 K is $\sim 2 \times 10^{-11} \text{ cm}^3 \text{ s}^{-1}$ (Messing *et al.* 1981). No laboratory measurements of the rate constant are available for $\text{C}_2 + \text{N}$; the estimate from Prasad and Huntress (1980) of $5 \times 10^{-11} \text{ cm}^3 \text{ s}^{-1}$ at 300 K is used here. A temperature dependence of $(T/300 \text{ K})^{0.5}$ is assumed for these reactions because of the possibility of activation energies. The two neutral-neutral reactions, in the above proportion, are incorporated into the chemical model displayed in Figure 4 and discussed further below. Production via ion-molecule reactions is dismissed as unimportant.

In summary, the most important channel for the production of CN appears to be the one with neutral-neutral reactions. *The CN radical thus is the first observable molecule with a heavy atom that requires neutral-neutral reactions for its formation in diffuse clouds; the other molecules, i.e., CH, CH^+ , CO, and probably OH, are understood in terms of production mechanisms involving ion-molecule reactions (e.g., Federman *et al.* 1980; Danks, Federman, and Lambert 1984). If $\text{C}_2 + \text{N}$ dominates, as is necessary to reproduce the steep dependence of CN on H_2 , then CN is a third-generation neutral molecule: $\text{CH} \rightarrow \text{C}_2 \rightarrow \text{CN}$. The CN radical is the first such molecule measured in diffuse clouds ($A_V \lesssim 1 \text{ mag}$).*

c) Destruction of CN

Photodissociation by ultraviolet photons is a major destruction process for molecules in diffuse clouds. Since in these clouds CN appears to be a third-generation, neutral molecule, three photodestruction terms enter into the rate equation for

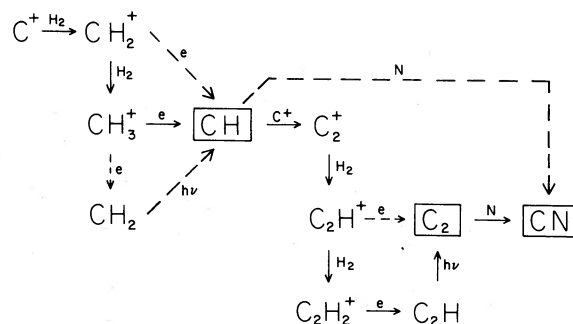


FIG. 4.—The gas phase chemistry leading to the production of CN. Channels of lesser importance are shown by dashed lines. Destruction of CH, C_2 , and CN occurs primarily by photodissociation (not shown).

CN, one term each from CH, C_2 , and CN. Thus, the attenuation factor that accompanies the photodestruction includes the sum of three optical depths, indicating a strong exponential dependence for the column density of CN on the UV optical depth of the cloud. (Eq. [1] also illustrates the strong density dependence expected from a molecule like CN.) At higher gas densities and in the inner regions of the most opaque clouds, gas phase reactions may compete with photodissociation.

d) Predicted CN Column Density

The reaction network in Figure 4 leads to the following relation between the column densities of CN, C_2 , and CH:

$$N(\text{CN}) = [N(\text{C}_2) + \frac{2}{5}N(\text{CH})]k(T/300)^{0.5} \times x(\text{N})n/(G_{\text{CN}}^0 \exp[-\tau_{\text{CN}}]) \text{ cm}^{-2}, \quad (2)$$

where k is the rate constant at 300 K for the neutral-neutral reaction $\text{C}_2 + \text{N} \rightarrow \text{CN} + \text{C}$. The abundance of gaseous nitrogen is taken to be $x(\text{N}) = 4.5 \times 10^{-5}$, i.e., depleted by a factor of 2 relative to its total (i.e., solar) abundance (York *et al.* 1983). The photodissociation rate is set equal to the value used by Black and Dalgarno (1977), $G_{\text{CN}}^0 = 5 \times 10^{-11} \text{ s}^{-1}$, and τ_{CN} is the optical depth due to grains. The local gas density n appears in equation (2) because we write $n(\text{N}) = x(\text{N})n$. In order to effect a comparison with observations, we replace certain volume densities by column densities; i.e., $N(\text{CN})$ and $N(\text{C}_2)$ for $n(\text{CN})$ and $n(\text{C}_2)$. This is valid as long as the clouds are not highly structured.

The relation between the CN and H_2 densities is completed with the equations

$$N(\text{CH}) = 0.67k_5x(\text{C}^+)nN(\text{H}_2)/[G_{\text{CH}}^0 \exp[-\tau_{\text{CH}}] + k_3x(\text{C}^+)n] \text{ cm}^{-2} \quad (3)$$

and

$$N(\text{C}_2) = k_3x(\text{C}^+)nN(\text{CH})/[G_{\text{C}_2}^0 \exp[-\tau_{\text{C}_2}] + k'x(\text{O})n] \text{ cm}^{-2}, \quad (4)$$

where k_3 is the rate constant for $\text{CH} + \text{C}^+ \rightarrow \text{C}_2^+ + \text{H}$, k_5 is the rate constant for $\text{C}^+ + \text{H}_2 \rightarrow \text{CH}_2^+ + h\nu$ (see Federman 1982), and k' is the rate constant for $\text{C}_2 + \text{O} \rightarrow \text{CO} + \text{C}$. At the highest densities and optical depths modeled below, gas phase reactions compete with photodissociation. Observations show that for diffuse clouds with $N(\text{H}_2) \gtrsim 3.5 \times 10^{20} \text{ cm}^{-2}$, $N(\text{C}_2)$ often exceeds $N(\text{CH})$ so that $N(\text{C}_2)$ dominates in the first term in equation (2).

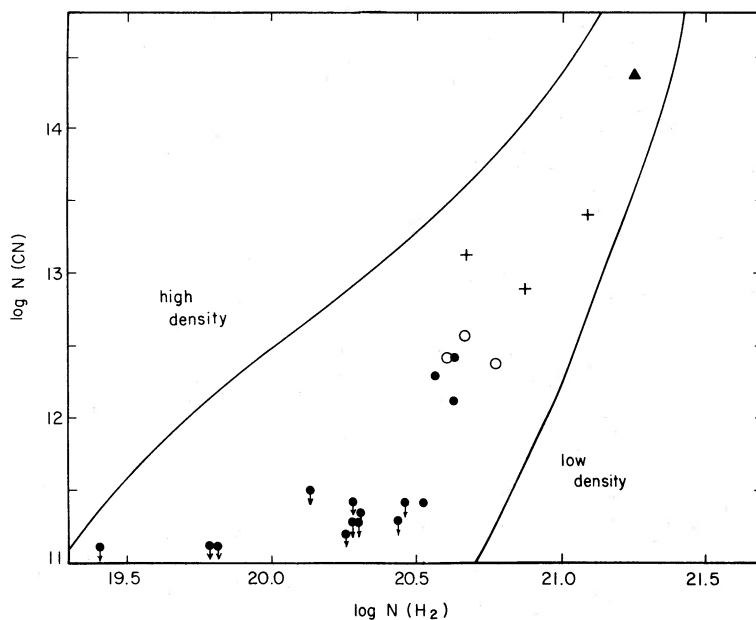


FIG. 5.—Predictions and observations in the $\log N(\text{CN})$ – $\log N(\text{H}_2)$ plane. The two solid curves are the results of the theoretical models described in the text. The data points are from the observations reported here (filled circles) and published observations (open circles for σ Per, ζ Per and λ Cep, crosses for χ Per, HD 154368, and 20 Aql, and a triangle for HD 29647). The column densities are expressed in the units molecules cm^{-2} .

Predictions from the full reaction network (Fig. 4) and the observations (Table 1) are compared in Figure 5. The two predictions refer to low- and high-density clouds. The low-density case has an average density of $n = 150 \text{ cm}^{-3}$ and an average temperature of $T = 55 \text{ K}$; for the high density case, the average parameters are respectively $n = 2500 \text{ cm}^{-3}$ and $T = 30 \text{ K}$. These two cases represent the typical range of parameters used to describe the diffuse clouds analyzed here.

Indeed, the CN observations fall about midway between the curves. This result was also found when CO and CH were analyzed with the models (Federman *et al.* 1980; and Danks, Federman, and Lambert 1984, respectively). Physical parameters intermediate between the values chosen for our two calculations probably are representative for diffuse clouds with molecular line absorption. A density of approximately 500 – 1000 cm^{-3} and a temperature around 50 – 60 K seem quite reasonable. Such values for the density and temperature are consistent with the observational results of Crutcher and Watson (1981) for the gas toward ζ Ophiuchi and of Savage *et al.* (1977) for all the directions with detectable amounts of CN. Crutcher and Watson (1981) based their analysis on the ratio of ^{12}CO to ^{13}CO ; Savage *et al.* (1977) determined the rotational temperature of H_2 .

The observations more closely follow the slope of the low-density curve rather than the high-density curve. The former curve has the slope expected when photodissociation is the dominant mode of destruction. The high-density models provide a more gradual increase of $N(\text{CN})$ with $N(\text{H}_2)$ because gas-phase reactions like $\text{C}^+ + \text{CH}$ compete with photodestruction in these model clouds. At densities of about 500 cm^{-3} , the $\text{C}^+ + \text{CH}$ reaction is as important as photodestruction, but neutral-neutral reactions are important at the highest densities considered here only when $A_V \lesssim 1 \text{ mag}$. In the extreme case where gas phase reactions dominate destruction, $N(\text{CN})$ varies approximately as $N(\text{H}_2)$, clearly discordant with the observations.

At present, definition of the CN– H_2 relation beyond the

maximum H_2 column density represented in Table 1 and Figure 5 is impossible because observations of the H_2 lines are unavailable and unattainable. A few observations of the CN lines have been published for lines of sight for which $N(\text{H}_2)$ most probably exceeds $5 \times 10^{20} \text{ cm}^{-2}$. Dickman *et al.* (1983) have compiled a catalog of CN observations. We extracted from this list the stars with $N(\text{CN}) \gtrsim 10^{13} \text{ cm}^{-2}$. When published W_λ 's were available, we recomputed $N(\text{CN})$. A preliminary estimate of $N(\text{H}_2)$ is provided by Bohlin, Savage, and Drake's (1978) relation between the reddening E_{B-V} and the total hydrogen column density $N(\text{H}_{\text{tot}}) = N(\text{H I}) + 2N(\text{H}_2)$ and by the assumption that $f = 2N(\text{H}_2)/N(\text{H}_{\text{tot}}) \approx 0.5$ in these rather reddened lines of sight (see Savage *et al.* 1977). Data points for three lines of sight— χ Per, HD 154368, and 20 Aql—may be added to Figure 5 by this process. Crutcher (1984) has analyzed the interstellar spectrum of the heavily reddened ($A_V = 3.7 \text{ mag}$) star HD 29647. We note that the four additional points lie on an extension of the previously established relation.

A more severe test of the proposed scheme for the formation and destruction of CN is possible for a few well-studied lines of sight for which column densities of the key molecules—CN, CH, and C_2 —have been measured. Use of the observed column densities of CH and C_2 ensures that the test is essentially independent of deficiencies in the modeling of the reaction works by which CH and C_2 are formed from H_2 and H. Measured column densities for HD 29647 were taken from Crutcher (1984); his $N(\text{CN})$ and $N(\text{C}_2)$ were adjusted to be compatible with the oscillator strengths adopted here and in Danks and Lambert (1983). For HD 154368, we took the CN density from our recalculation (see above), the CH column density from Dickman *et al.* (1983), the C_2 column density from van Dishoeck and de Zeeuw (1984) and corrected it to the oscillator strength adopted by Danks and Lambert (1983); the CH estimate is uncertain because of the severe saturation of the 4300 \AA line. Values of $N(\text{CH})$ and $N(\text{C}_2)$ for the other lines of sight are provided by Danks and Lambert (1983).

TABLE 2
OBSERVED AND PREDICTED COLUMN DENSITIES

STAR	OBSERVED $N(AB)$ [cm^{-2}]			PREDICTED $N(\text{CN})$ [cm^{-2}]
	$N(\text{CH})$	$N(\text{C}_2)$	$N(\text{CN})$	Neutral-Neutral ^a
σ Per	1.3(13)	2.7(13)	2.6(12)	2.0(12)
ζ Per	1.8(13)	3.5(13)	3.9(12)	2.4(12)
HD 29647	1.7(14)	9.0(13)	1.9(14)	5.3(13)
ρ Oph	1.9(13)	2.6(13)	2.0(12)	4.0(12)
χ Oph	2.5(13)	3.5(13)	1.3(12)	2.7(12)
ζ Oph	2.3(13)	2.2(13)	2.6(12)	1.8(12)
HD 154368	2.6(14)	5.8(13)	2.6(13)	3.3(13)

^a Predictions for the reaction in which CN is formed by neutral-neutral reactions from C_2 and CH (see Fig. 4).

Predictions for the neutral-neutral chemistry in which CN is formed from C_2 and CH are based on equation 2, the numerical estimates discussed previously, and the observed column densities of C_2 and CH. The physical parameters, density and temperature, for HD 154368 and the stars in Perseus and Ophiuchus (except χ Oph) were set at $n = 500 \text{ cm}^{-3}$ and $T \approx 50\text{--}60 \text{ K}$ (e.g., Crutcher and Watson 1981); $n = 250 \text{ cm}^{-3}$ and $T = 45 \text{ K}$ (van Dishoeck and de Zeeuw 1984) were adopted for χ Oph. We adopt $n = 1500 \text{ cm}^{-3}$ and $T = 10 \text{ K}$ for HD 29647 (Crutcher 1984) and $n = 250 \text{ cm}^{-3}$ and $T = 25 \text{ K}$ for HD 154368 (van Dishoeck and de Zeeuw 1984). The optical depth τ_{CN} was taken to be $2A_v$. For the more reddened lines of sight, a correction for the destruction of CN by $\text{CN} + \text{O} \rightarrow \text{CO} + \text{N}$ is necessary. This correction was substantial for HD 29647 (a factor of 10) and HD 154368 (a factor of 2) but was less than 30% for other lines of sight. It should be noted that the lines of the sight toward HD 29647 and HD 154368 have more extinction than a typical diffuse cloud ($A_v \leq 1 \text{ mag}$).

Predicted CN column densities for the neutral-neutral reaction network match the observed column densities to within a factor of 2 (see Table 2), and generally much better, except for HD 29647, the cloud with the highest density and opacity. Such quantitative agreement suggests that the neutral-neutral reaction $\text{C}_2 + \text{N} \rightarrow \text{CN} + \text{C}$ dominates the formation of CN in diffuse clouds. If CN formation were restricted to the alternative route $\text{CH} + \text{N} \rightarrow \text{CN} + \text{H}$, the predicted CN column densities are a factor of almost 10 too small for σ Per, ζ Per, and HD 29647, a factor of 5 too small for ζ Oph, and a factor of 2 too small for ρ Oph. For χ Oph and HD 154368 CH can account for the observed CN column density. Since the $\text{CH} + \text{N}$ rate constant has been measured, these predicted CN column densities cannot be adjusted upward by increasing the rate of CN formation by a factor of 5 to bring the predicted and observed CN column densities into rough agreement. However, this argument in favor of formation of CN from C_2 must be accompanied by the qualifying remark that the photodissociation rate for CN is not yet well determined and the adopted value could conceivably be too large by a factor of 5. Clearly, definitive determinations of this photodissociation rate and of the rate constant for $\text{C}_2 + \text{N} \rightarrow \text{CN} + \text{C}$ are needed

to complete the quantitative chemistry of interstellar CN. Our comparison of $N(\text{CN})$ and $N(\text{H}_2)$ in Figure 3 also suggests that $\text{C}_2 + \text{N} \rightarrow \text{CN} + \text{C}$ is the more important neutral-neutral reaction. If $\text{CH} + \text{N} \rightarrow \text{CN} + \text{H}$ were dominant, one would expect $\log N(\text{CN}) \propto m \log N(\text{H}_2)$ with $m = 2$ [similar to the relationship between $N(\text{CO})$ and $N(\text{H}_2)$], which is marginally excluded by the observations.

IV. CONCLUDING REMARKS

A search for interstellar CN lines along lines of sight with known H_2 column density uncovered the remarkable new result that the CN column density increases sharply with H_2 column density in diffuse clouds (Fig. 3). Inspection of the chemical reactions expected to produce (and remove) CN in neutral diffuse clouds shows that CN is a third-generation, neutral molecule with production occurring from C^+ and H_2 through ion-molecule reactions to C_2 and with the neutral-neutral reaction $\text{C}_2 + \text{N} \rightarrow \text{CN} + \text{C}$ completing the formation process of the CN radical. The neutral-neutral reaction $\text{CH} + \text{N} \rightarrow \text{CN} + \text{H}$ is of some importance for CN production. Photodissociation of CH, C_2 , and CN results in a strong dependence of $N(\text{CN})$ on gas density and optical depth, leading to rapid variation between CN and H_2 . The CN radical is the only third-generation, neutral molecule analyzed in diffuse clouds to date. With this studd of CN, modeling of carbon chemistry in diffuse clouds, which had earlier accounted quantitatively for the variation of C I (Jenkins and Shaya 1979; Jenkins, Jura, and Loewenstein 1983), CH (Federman 1982; Danks, Federman, and Lambert 1984) and CO (Federman *et al.* 1980) with H_2 column density, has not been extended successfully to CN.

We thank Dr. R. Crutcher for use of his unpublished data and the referee for several constructive comments. D. L. L. thanks the Kitt Peak National Observatory for a travel grant. D. L. L. and S. R. F. thank Dr. A. Ardeberg for hospitality on La Silla. S. R. F. acknowledges support as a NAS/NRC Research Associate while at the Jet Propulsion Laboratory. This research has been supported in part by grants from the National Science Foundation (AST 81-17485) and the Robert A. Welch Foundation of Houston, Texas.

APPENDIX

THE OSCILLATOR STRENGTH OF INTERSTELLAR CN LINES

Almost without exception, authors cite Herbig's (1968) thorough discussion of the interstellar line spectrum of ζ Oph when requiring an oscillator strength for the CN lines. Unfortunately, the value selected by Herbig is in need of revision.

An accurate measurement of the radiative lifetime $\tau_{v'}$ of the $B^2\Sigma^+$ state reported by Jackson (1974) provides a band oscillator strength $f_{v'v''}$: $f_{00} = 0.0342$ with an uncertainty of about 5% (see Lambert 1978). Jackson's lifetime $\tau_0 = 65.5 \pm 1.0$ ns, was confirmed by Đurić, Erman, and Larsson (1978) who obtained $\tau_0 = 66.2 \pm 0.8$ ns. Ab initio calculations reproduce these measurements (Larsson, Siegbahn, and Ågren 1983). By contrast, Herbig adopted $f_{00} = 0.0173$, a full factor of 2 smaller than the above accurate result.

Conversion of the band oscillator strength $f_{v'v''}$ to the oscillator strength of an individual line $f_{J',J''}$ or blend of lines is apparently a source of an error in certain literature citations of the CN column density. The key relation (Larsson 1983) is

$$\begin{aligned} f_{J',J''} &= (2 - \delta_{0,\Lambda'}) / (2 - \delta_{0,\Lambda'+\Lambda''}) f_{v'v''} S_{J',J''} / (2J'' + 1) \\ &= f_{v'v''} S_{J',J''} / (2J'' + 1) \end{aligned}$$

for the CN violet system where the Hönl-London factor $S_{J',J''}$ is subject to the sum rule

$$\begin{aligned} \sum_{J'} S_{J',J''} &= (2 - \delta_{0,\Lambda'+\Lambda''}) (2S + 1) (2J'' + 1) \\ &= 2(2J'' + 1) \end{aligned}$$

with the summation covering the transitions R_1 , R_2 , ${}^R Q_{21}$, P_1 , ${}^P Q_{12}$, and P_2 . Expressions for $S_{J',J''}$ are provided by several authors but may not be normalized according to the above sum rule; e.g., Schadee's (1964) expressions must be multiplied by 2.

The strongest line from the lowest level ($N'' = 0$, $J'' = \frac{1}{2}$) in the vibrational ($v'' = 0$) state of the $X^2\Sigma^+$ state is a blend of the $R_1(0)$ and ${}^R Q_{21}(0)$ lines with Hönl-London factors of $S(R_1) = \frac{4}{3}$ and $S({}^R Q_{21}) = \frac{2}{3}$. The blend has, as it must, an oscillator strength $f_{J',J''} = f_{v'v''} = 0.0342$. We ignore the hyperfine components and assume that the two hyperfine levels of the $N'' = 0$ level are in thermal equilibrium.

The line $R(1)$ is a blend of three components: $R_1(1) + {}^R Q_{21}(1) + R_2(1)$. The $N'' = 1$, $J'' = \frac{1}{2}$ level provides $R_2(1)$ with $S_{J',J''} / (2J'' + 1) = \frac{2}{3}$. The other two lines from the $N'' = 1$, $J'' = \frac{3}{2}$ level have a combined $S_{J',J''} / (2J'' + 1) = \frac{2}{3}$. The two $N'' = 1$ levels are separated by only 0.011 cm^{-1} (or 0.016 K). The unresolved trio of lines has an equivalent width

$$\begin{aligned} W_\lambda &= \pi e^2 / (mc^2) \lambda^2 \frac{2}{3} f_{v'v''} [N(J'' = \frac{1}{2}) + N(J'' = \frac{3}{2})] \\ &= \pi e^2 / (mc^2) \lambda^2 \frac{2}{3} f_{v'v''} N(N'' = 1), \end{aligned}$$

where $N(N'' = 1) = N(J'' = \frac{1}{2}) + N(J'' = \frac{3}{2})$, i.e., an effective oscillator strength of $\frac{2}{3} f_{v'v''} = 0.0228$. A similar analysis shows that the $P_1(1) + {}^P Q_{12}(1)$ blend has, of course, an effective oscillator strength $f = \frac{1}{3} f_{v'v''}$.

Application of these results to ζ Oph where $R(0)$ has $W_\lambda = 7.5 \pm 0.3 \text{ mÅ}$ ($W_\lambda = 8.3 \pm 0.4 \text{ mÅ}$ after correction for saturation) and $R(1)$ has $W_\lambda = 2.6 \pm 0.3 \text{ mÅ}$ yields

$$N(N'' = 1) / N(N'' = 0) = 0.47 \pm 0.08,$$

which compares with a population ratio of 0.43 at an excitation temperature of $T_{\text{exc}} = 2.8 \text{ K}$. Herbig (1968)'s results are often quoted for ζ Oph (see, for example, Morton 1975) but he gives $N(N'' = 1) \approx N(N'' = 0)$ even though he states that the population ratio corresponds to $T_{\text{exc}} = 3.1$. The source of the confusion appears to be in the ratio of the oscillator strength adopted for $R(1)$ and $R(0)$. With our oscillator strengths, our W_λ for $R(0)$, and an assumed $T_{\text{exc}} = 2.8 \text{ K}$, the total CN column density is $N(\text{CN}) = 2.7 \times 10^{12} \text{ cm}^{-2}$, not the $8.7 \times 10^{12} \text{ cm}^{-2}$ given by Herbig.

REFERENCES

- Black, J. H., and Dalgarno, A. 1973, *Ap. Letters*, **15**, 79.
 ———. 1977, *Ap. J. Suppl.*, **34**, 405.
 Black, J. H., Dalgarno, A., and Oppenheimer, M. 1975, *Ap. J.*, **199**, 633.
 Blades, J. C., Wynne-Jones, I., and Wayte, R. C. 1980, *M.N.R.A.S.*, **193**, 849.
 Bohlin, R. C., Savage, B. D., and Drake, J. F. 1978, *Ap. J.*, **224**, 132.
 Bortolot, V. J., Jr., Clauser, J. F., and Thaddeus, P. 1969, *Phys. Rev. Letters*, **22**, 307.
 Chaffee, F. H., Jr. 1974, *Ap. J.*, **189**, 427.
 Chaffee, F. H., Jr., and Dunham, T., Jr. 1979, *Ap. J.*, **233**, 568.
 Clauser, J. F., and Thaddeus, P. 1972, in *Topics in Relativistic Astrophysics* (New York: Gordon and Breach).
 Crutcher, R. M. 1984, *Ap. J.*, submitted.
 Crutcher, R. M., and Watson, W. D. 1976, *Ap. J.*, **209**, 778.
 ———. 1981, *Ap. J.*, **244**, 855.
 Danks, A. C., Federman, S. R., and Lambert, D. L. 1984, *Astr. Ap.*, **130**, 62.
 Danks, A. C., and Lambert, D. L. 1983, *Astr. Ap.*, **124**, 188.
 Dickman, R. L., Somerville, W. B., Whittet, D. C. B., McNally, D., and Blades, J. C. 1983, *Ap. J. Suppl.*, **53**, 55.
 Đurić, N., Erman, P., and Larsson, M. 1978, *Phys. Scripta*, **18**, 39.
 Elitzur, M., and Watson, W. D. 1978, *Ap. J. (Letters)*, **222**, L141.
 ———. 1980, *Ap. J.*, **236**, 172.
 Enard, D. 1979, *Messenger*, No. **17**, p. 32.
 Federman, S. R. 1982, *Ap. J.*, **257**, 125.
 Federman, S. R., Glassgold, A. E., Jenkins, E. B., and Shaya, E. J. 1980, *Ap. J.*, **242**, 545.
 Frisch, P. 1979, *Ap. J.*, **227**, 474.
 Glassgold, A. E., and Langer, W. D. 1976, *Ap. J.*, **206**, 85.
 Hegyi, D. J., Traub, W. A., and Carleton, N. P. 1972, *Phys. Rev. Letters*, **28**, 1541.
 Herbig, G. H. 1968, *Zs. Ap.*, **68**, 243.
 Jackson, W. M. 1974, *J. Chem. Phys.*, **61**, 4177.
 Jenkins, E. B., and Shaya, E. J. 1979, *Ap. J.*, **231**, 55.
 Jenkins, E. B., Jura, M., and Loewenstein, M. 1983, *Ap. J.*, **270**, 88.
 Lambert, D. L. 1978, *M.N.R.A.S.*, **182**, 249.
 Larsson, M. 1983, *Astr. Ap.*, **128**, 291.
 Larsson, M., Siegbahn, P. E. M., and Ågren, H. 1983, *Ap. J.*, **272**, 369.
 Liszt, H. S. 1979, *Ap. J. (Letters)*, **233**, L146.
 Messing, I., Filseth, S. V., Sadowski, C. M., and Carrington, T. 1981, *J. Chem. Phys.*, **74**, 3874.
 Meyer, D. M., and Jura, M. 1984, *Ap. J. (Letters)*, **276**, L1.
 Middleburg, F. 1981, IHAP Users' Manual.
 Morton, D. C. 1975, *Ap. J.*, **197**, 85.
 Prasad, S. S., and Huntress, W. T., Jr. 1980, *Ap. J. Suppl.*, **43**, 1.
 Savage, B. D., Bohlin, R. C., Drake, J. F., and Budich, W. 1977, *Ap. J.*, **216**, 291.

Schadee, A. 1964, *Bull. Astr. Inst. Netherlands*, **17**, 311.

Strömberg, B. 1948, *Ap. J.*, **108**, 242.

Thaddeus, P. 1972, *Ann. Rev. Astr. Ap.*, **10**, 305.

Tull, R. G., Choisser, J. P., and Snow, E. H. 1975, *Appl. Optics*, **14**, 1182.

van Dishoeck, E. F., and de Zeeuw, T. 1984, *M.N.R.A.S.*, **206**, 383.

Viggiano, A. A., Howorka, F., Albritton, D. L., Fehsenfeld, F. C., Adams, N. G., and Smith, D. 1980, *Ap. J.*, **236**, 492.

York, D. G., Spitzer, L., Bohlin, R. C., Hill, J., Jenkins, E. B., Savage, B. D., and Snow, T. P., Jr. 1983, *Ap. J. (Letters)*, **266**, L55.

A. C. DANKS: European Southern Observatory, Casilla 19001, Santiago 19, Chile

S. R. FEDERMAN: Jet Propulsion Laboratory, 4800 Oak Grove Drive, Pasadena, CA 91109

D. L. LAMBERT: Department of Astronomy, University of Texas, Austin, TX 78712